Structural and magnetic properties of V/Co_{fcc} and Co_{hcp}/V bilayers grown on MgO(100): A comparative study

J. F. Calleja[a)]
Departamento de Física, Facultad de Ciencias, Universidad de Oviedo, Calvo Sotelo s/n, 33007 Oviedo, Spain

Y. Huttel
Instituto de Ciencia de Materiales de Madrid (ICMM-CSIC), Cantoblanco, 28049 Madrid, Spain

M. C. Contreras
Departamento de Física, Facultad de Ciencias, Universidad de Oviedo, Calvo Sotelo s/n, 33007 Oviedo, Spain

E. Navarro
Departamento de Física de Materiales, Facultad de Físicas, Universidad Complutense, 28040 Madrid, Spain

B. Presa and R. Matarranz
Departamento de Física, Facultad de Ciencias, Universidad de Oviedo, Calvo Sotelo s/n, 33007 Oviedo, Spain

A. Cebollada
Instituto de Microelectrónica de Madrid-IMM (CNM-CSIC), Isaac Newton 8 (PTM), Tres Cantos, 28760 Madrid, Spain

(Received 6 November 2005; accepted 20 July 2006; published online 15 September 2006)

A detailed study of the structure and magnetic properties of V/Co versus Co/V bilayers grown on MgO(001) substrates with cubic and hexagonal Co crystal structures is presented. Co is found to adopt fcc structure when grown on MgO(001), while it adopts hcp structure when grown on V(001). The different magnetocrystalline anisotropy associated with each structure gives rise to different magnetic properties for the otherwise equivalent symmetric Co–V bilayers. © *2006 American Institute of Physics*. [DOI: 10.1063/1.2336496]

I. INTRODUCTION

Of increasing importance in modern technology are magnetic thin films and interfaces involving thin films. On the one hand, effects usually neglected in three dimensional systems may become important as the dimensions of the system perpendicular and parallel to the film surface become very different. On the other hand, the interface is believed to play an important role in, for example, the oscillatory magnetic coupling that is essential for the giant magnetoresistance phenomenon. Magnetic anisotropy is a key parameter in ferromagnetic thin film behavior since it helps to determine the coercivity and the magnetization reversal process. At the same time, the magnetic anisotropy depends on the microscopic structure of the system, in particular in epitaxial films. Moreover, the film growth mode can give rise to the development of nanostructures (islands) in the first steps of the film growth that have a great impact on the magnetic anisotropy.

In the last decade great attention has been paid to the study of V/Co multilayers [1–4] due to the oscillatory exchange through V layers. These studies clearly indicated that a better understanding of the interface magnetism at the V/Co interface is mandatory to understand the physics of this system. The orientation of the magnetization in a ferromagnetic thin film is determined by the competition between different parameters such as shape anisotropy, magnetocrystalline anisotropy, magnetic surface anisotropy, epitaxial strain, etc.[5] The structures of Co [body centered cubic (bcc), face centered cubic (fcc), and hexagonal close packed (hcp)] provide excellent model systems for the study of the influence of the magnetocrystalline anisotropy on the interface anisotropy and its role in the induction of magnetic moment in the V atoms.

In this paper we present a comparative study of the structure, magnetic properties and magnetic anisotropies of the V–Co system formed in two different stacking sequences, namely, Co/V/MgO(100) and V/Co/MgO(100). These sequences give rise to different Co crystalline structures (hcp versus fcc) and therefore to different magnetic behaviors. The paper is organized as follows: In Sec. II we briefly present the experimental details; In Sec. III we present the experimental results including x-ray diffraction, transverse Kerr, and transverse susceptibility results. In Sec. IV we discuss the results and then present the conclusions.

II. EXPERIMENTAL PROCEDURE

The samples were grown in a combined ultrahigh vacuum system (base pressure in the low 10^{-9} mbar) with triode sputtering and laser ablation facilities. The Co and V films were deposited by triode sputtering onto MgO(100)

a)Electronic mail: jfcalleja@uniovi.es

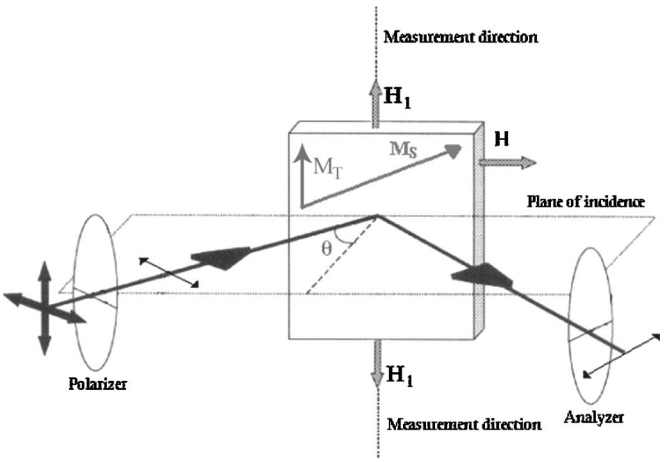

FIG. 1. Geometry of the magneto-optical experimental setup used for the measurement of the transverse susceptibility and hysteresis loops. The transverse component of the magnetization M_t is measured as a function of H_1 (hysteresis loop) or as a function of H (transverse susceptibility).

single crystals at normal incidence. The argon pressure during the sputtering was kept at 4×10^{-4} mbar and the deposition rates were in the range of a few Å/min. Prior to V and Co deposition, an 80 Å MgO buffer layer was grown by laser ablation at 450 °C on the substrate to planarize the surface. Subsequent to the room temperature (RT) deposition of the V and Co, a 30 Å thick Al capping layer was deposited at RT in order to protect the films from oxidation. Different Co crystalline structures were obtained by inverting the deposition sequence of V and Co. As the magnetic anisotropy of the system under study is expected to be mainly determined by the Co crystallographic structure and the Co layer thickness, the samples were tailored as follows. In the case of fcc Co/MgO(001), three systems were investigated: Al/100 Å Co/MgO, Al/20 Å Co/MgO, and Al/15 Å V/20 Å Co/MgO. The last one was chosen in order to investigate the influence of a possible V polarization. In the case of hcp Co/V, the systems under investigation were Al/200 Å Co/40 Å V/MgO and Al/20 Å Co/40 Å V/MgO, with the Co thickness as the varying parameter.

Crystallographic structure, transverse Kerr loops, and magnetic anisotropy were measured after the samples were removed from the vacuum system. The crystallographic structure was investigated using x-ray diffraction (XRD) with a four-circle diffractometer, Cu $K\alpha$ radiation, and 1/4° divergence slits. Both symmetric ($\theta/2\theta$ scans) and asymmetric phi scans (φ scans) have been recorded. The asymmetric phi scans have been recorded selecting an off normal diffraction peak (either from the V or the Co layers) and rotating the sample around its surface normal. This allows us to determine the crystallographic symmetry (if it exists) in the plane of the surface of the structure under study.

The magnetic anisotropy was obtained from transverse susceptibility (TS) measurements which are performed using the transverse magneto-optical Kerr effect. The experimental setup used to obtain the hysteresis loops and the TS is shown in Fig. 1. Two magnetic fields, H_1 and H, can be applied in the plane of the sample. In order to obtain a hysteresis loop only a low frequency magnetic field H_1 is applied. In the

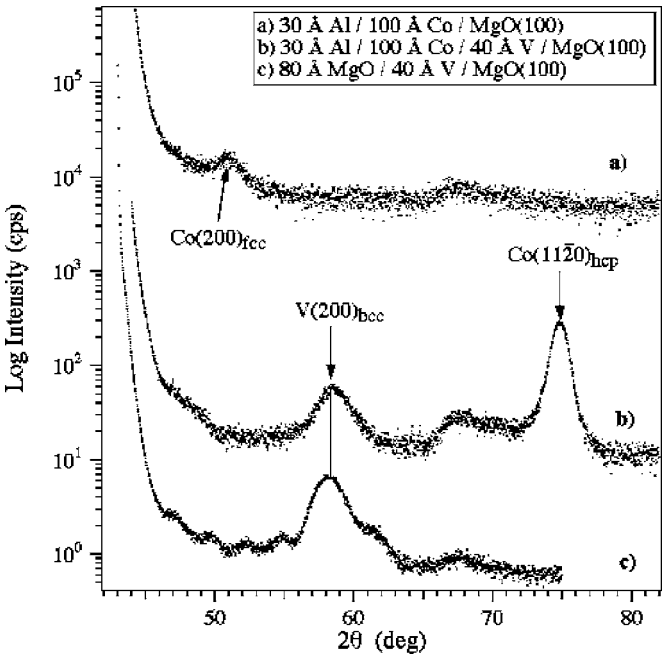

FIG. 2. Selected symmetric XRD scans for the V/MgO(100), Co/MgO(100), and Co/V/MgO(100) structures.

case of transverse susceptibility measurements two magnetic fields are applied: H_1, which in this case is a small amplitude alternating field (the frequency of H_1 used was 127 Hz), and an orthogonal bias field H, both in the film plane. These magnetic fields are produced by two pairs of Helmholtz coils perpendicular to each other. The light from the light source is linearly polarized with the electric vector in the plane of incidence. The magneto-optic Kerr effect produces a small change in the intensity of the reflected light proportional to the component of the magnetization perpendicular to the plane of incidence M_t. The light detected in the photodiode changes accordingly. If the amplitude of H_1 is small enough, the Kerr signal is proportional to the susceptibility, and we obtain the transverse susceptibility as a function of the bias field H. In order to carry out the magnetic characterization of the samples, TS measurements are performed with H applied along different directions, as explained in the following paragraphs. The direction of the sample relative to the magnetic fields is controlled by rotating the sample holder. All the measurements were performed at room temperature.

III. RESULTS

A. X-ray diffraction

The crystallographic structure of the samples has been investigated by means of x-ray diffraction. Both symmetric ($\theta/2\theta$ scans) and asymmetric phi scans (φ scans) have been recorded and the corresponding spectra are displayed in Figs. 2 and 3. Figure 2 displays the symmetric scans for both Co/V/MgO(100) and Co/MgO(100) systems. For reference, we present at the bottom of Fig. 2 the diffraction scan corresponding to 40 Å of V grown on MgO(100) and capped with MgO layer. The intense tail below 50° comes from the MgO(200) diffraction peak. As reported previously[6] the feature located at around 58° corresponds to the V(200) diffrac-

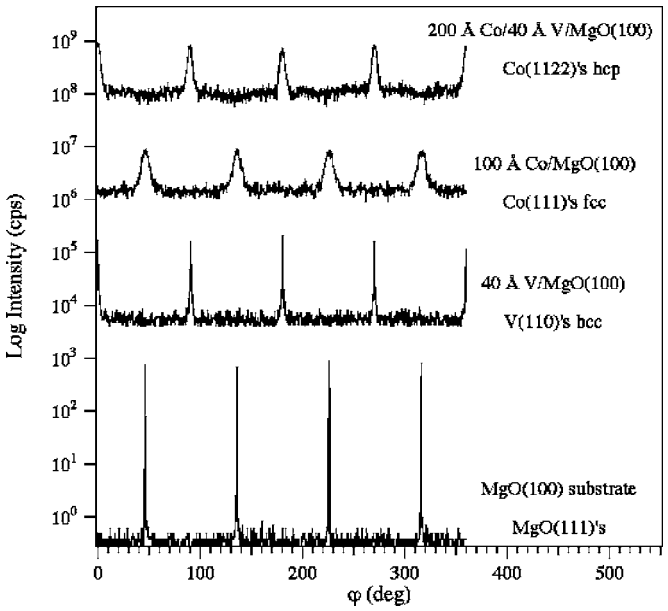

FIG. 3. Representative asymmetric φ scans for MgO(111), V(110), Co(111), and Co($11\bar{2}2$) reflections for different structures grown on MgO(100) substrates. The φ scans illustrate the epitaxial relationships that govern the growth of the structures. See text for details.

tion peak of the body centered cubic V structure. The crystallographic structure of the Co layer deposited on the V layer is illustrated through the scan corresponding to the 30 Å Al/100 Å Co/40 Å V/MgO(100) system. The feature located at 74.8° corresponds to the hcp Co($11\bar{2}0$) diffraction peak, indicating the growth of Co on V in the hcp structure[7] with the *c* axis located in the plane of the surface. As can be observed in Fig. 2, the growth of 100 Å of Co on MgO(100) results in the fcc structure, as revealed by the Co(200) diffraction peak located at 50.8° in the diffraction scan of the 30 Å Al/100 Å Co/MgO(100) sample. Unfortunately, the crystal structure of V on fcc Co in the 30 Å Al/15 Å V/20 Å Co/MgO sample could not be determined, as no signal was detected due to the small amount of V in the sample.

Further characterization of the crystallographic structure is given by the asymmetric φ scans displayed in Fig. 3. As can be observed in the asymmetric φ scan corresponding to the MgO(111) diffraction peak, the MgO substrates display the expected fourfold symmetry. As previously reported,[6,8–10] V grown on MgO(100) also displays a fourfold symmetry with an additional rotation of 45°, leading to the $V(001)_{bcc}[100]\|MgO(001)[110]$ epitaxial relation, i.e., a 45° in-plane rotation of the V[100] directions with respect to the MgO ones. On the other hand, it can be observed that the fcc Co grown on MgO(100) shows a well defined fourfold symmetry that corresponds to the following epitaxial relationship $Co(001)_{fcc}[100]\|MgO(001)[100]$ similar to the one reported for the growth of Co on MgO(100) at 250 °C.[11] As displayed in Fig. 2, when Co is deposited on the initial V/MgO(001) substrate, a Co hcp structure is formed with the *c* axis in the plane of the film. In Fig. 3 the Co($11\bar{2}2$) reflection shows a fourfold symmetry. This is due to the growth of Co($11\bar{2}0$) by simultaneous nucleation of crystalline domains with the (0001) axis aligned with equal probability along the V[100] and [010] directions, and therefore rotated 90° with respect to each other[6] similar to the Co/Mo/MgO(001) system.[12] In this case, the epitaxial relationship for both domains is $Co_{hcp}(11\bar{2}0\|V(001)\|MgO(001)$ for the growth direction, and $Co_{hcp}[0001]\|V[100]\|MgO[110]$ and $Co_{hcp}[0001]\|V[010]\|MgO[1\bar{1}0]$ for the two in-plane orientations. Also it can be noted that the Co($11\bar{2}2$) reflections of the corresponding φ scan have similar intensities, indicating that there are approximately equal volumes of the two hcp Co orientations.

B. Transverse Kerr

Kerr hysteresis loops have been recorded in the transverse geometry, i.e., with the magnetic field in the plane of the sample and perpendicular to the plane of incidence of the light. This geometry allows the measurement of the in-plane magnetization. Panels (a) and (b) of Fig. 4 display the representative Kerr hysteresis loops measured along the $[110]_{MgO}$ and $[100]_{MgO}$ directions for the systems Co/MgO(100) and V/Co/MgO(100), whereas panels (c) and (d) display the Kerr hysteresis loops along the same directions for the Co/V/MgO(100) system. It is interesting to note that no uniaxial in-plane anisotropy could be clearly identified in opposition to similar systems such as fcc Co(110)/MgO(110), 200 Å hcp Co/V/MgO(110), 200 Å hcp Co/Cr/MgO(110), and 200 Å hcp Co/Mo/MgO(110).[13,14] This is simply because the samples were here grown on (001) oriented surfaces [(001) V and MgO], promoting growth with fourfold symmetry. We first concentrate on the Kerr hysteresis loops of the systems Co/MgO(100) and V/Co/MgO(100). Whereas the Kerr hysteresis loops measured at different angles on 100 Å fcc Co/MgO(100) displayed a clear fourfold magnetic symmetry (not shown here), that was not the case for the Kerr hysteresis loops of 20 Å fcc Co/MgO(100) and 15 Å V/20 Å fcc Co/MgO(100). As expected the 100 Å fcc Co/MgO(100) exhibits an easy magnetization axis along the $[110]_{Co}$ axis. The corresponding coercivity along the easy magnetization axis is found to be close to 15 Oe which is considerably lower than the one expected in a thin layer of fcc Co grown on Cu(100).[15] The nonobservation of a clear magnetic in-plane anisotropy for 20 Å fcc Co/MgO(100) and 15 Å V/20 Å fcc Co/MgO(100) might be due to the lack of full continuity of the Co layers, the morphology of which would make it impossible to observe the fcc Co characteristic magnetocrystalline anisotropy. This result suggests the growth of fcc Co islands on the MgO substrate. Additionally, we observe that the growth of 15 Å of V on 20 Å Co/MgO(100) does not significantly modify the coercivity.

We now turn to the Kerr hysteresis loops of the Co/V/MgO(100) system in panels (c) and (d) of Fig. 4. As expected, the Kerr hysteresis loops display a clear easy axis of magnetization along the $[110]_{MgO}$ axis which corresponds also to the *c* axis of the hcp cobalt grown on bcc V. The coercivities of the 200 Å Co/40 Å V/MgO(100) system measured along the $[110]_{MgO}$ and $[100]_{MgO}$ (137 and 96 Oe, respectively) are very similar to the coercivity measured in

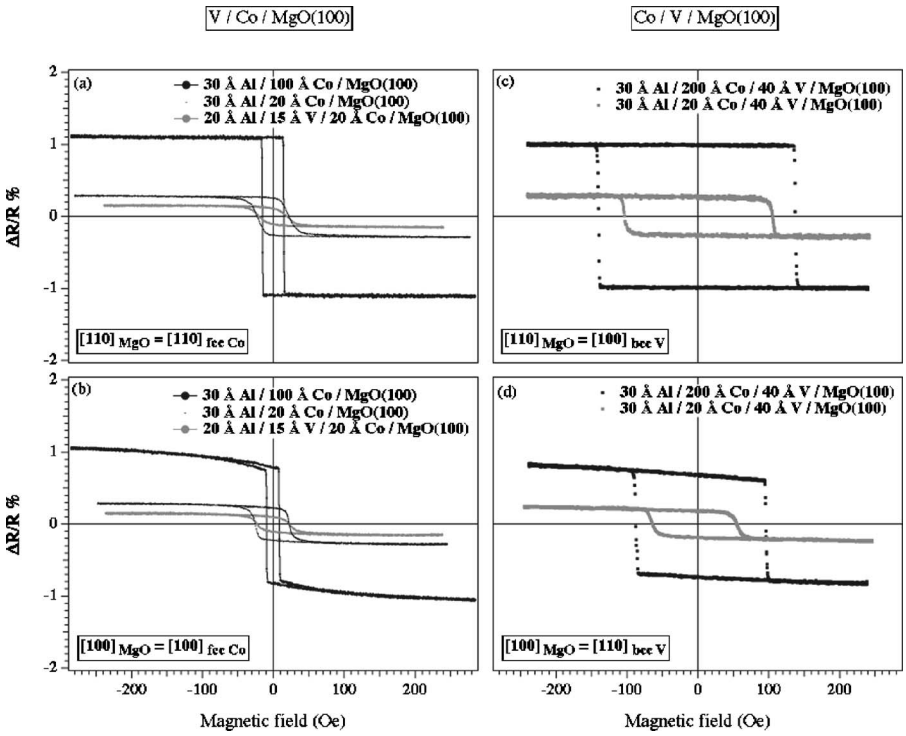

FIG. 4. Representative Kerr hysteresis loops measured in the transverse Kerr configuration for the Al/V/Co/MgO(100) and Al/Co/V/MgO(100) systems along both the $[110]_{MgO}$ and $[100]_{MgO}$ directions. Wavelength of light: 632.8 nm.

similar systems with the same hcp Co structure such as 200 Å Co hcp/Mo/MgO(100) (Ref. 16) and 200 Å Co/50 Å V/MgO(100) (Ref. 14) and much lower than that measured on a thick hcp Co film deposited on GaAs(001).[17] However, in disagreement with Lo *et al.*,[14] we did not observe a clear uniaxial magnetic anisotropy. The absence of uniaxial anisotropy indicates the presence of equal volumes of hcp Co crystals with easy directions 90° apart, leading to a fourfold in-plane magnetic symmetry. Such differences are probably due to the sample preparation, since it is well known that molecular beam epitaxy, electron beam epitaxy, and magnetron sputtering can lead to substantial differences in the growth mode of the evaporated species. Finally, the Co/V system with a thinner Co layer (20 Å Co/40 Å V/MgO) displays a less squared hysteresis loop than those observed for the systems formed with 200 Å of Co, as well as lower coercivities. Interestingly, in contrast to the 15 Å V/20 Å Co/MgO(100) system [panels (a) and (b)], the anisotropy is still observable with a strong reduction of the coercivity in the $[100]_{MgO}$ direction (55 Oe) compared to the $[110]_{MgO}$ direction (105 Oe).

C. Transverse susceptibility

TS measurements provide a fairly accurate description of the magnetic anisotropies involved in a system and a picture of the magnetization reversal mechanism along the direction in which the steady field H is applied. All these features are of interest in the systems under study. Moreover, we will show that TS measurements are much more sensitive than the hysteresis loop in describing these phenomena. In order to understand the information obtained from TS measurements, let us recall some general features of TS. Let us keep in mind that while the hysteresis loop is a representation of M_t vs H_1, TS is a representation of dM_t/dH_1 vs H. Any small change in the component of the saturation magnetization along H induces a small change in M_t which can be detected as a peak in the dM_t/dH_1. In order to understand the information obtained from TS measurements, let us consider the case of a single domain particle with uniaxial anisotropy in which only coherent magnetization rotation is to be considered. If K_u is the anisotropy constant and M_s the saturation magnetization, the anisotropy field is defined as $H_k=2K_u/M_s$. Applying the Stoner-Wohlfarth model,[18] we have calculated hysteresis loops and the corresponding TS for H_1 and H along the hard and easy axes. The results are shown in Fig. 5 (see also Ref. 19). The normalized applied field in Fig. 5 is, following the notation in Fig. 1, $h=H_1/H_k$ for the hysteresis loops [Figs. 5(a) and 5(c)] and $h=H/H_k$ for the TS [Figs. 5(b) and 5(d)]. The calculated TS exhibits singularities at $h=\pm 1$. In real single domain films such singularities become maxima in the detected signal and the position of the maximum for H along the easy axis occurs not for $h=-1$ as in Fig. 5(b) but for the field at which the magnetization reverses, i.e., at the coercive field H_c.[19] Both for H along the easy axis and for H along the hard axis, the inverse of the TS depends linearly on H for high fields for which the sample is saturated.[20,21] The case of a single domain particle with biaxial anisotropy has also been studied theoretically[22] and experimentally.[23] The behavior is similar to the previous one when H is applied either along the easy axis or along the hard axis: a maximum is detected in the former case for $H=-H_c$ and two maxima are detected in the latter case for $h=\pm 1$. The TS in this case also depends linearly on H for high H values.[21] The behavior of the TS is different in the case of particulate media. For thin films, both continuous granular and discontinuous films can be considered as particulate media, the particles being the crystallites in the former case and the islands in the latter case. In those cases, when H is applied along a hard axis two peaks in the

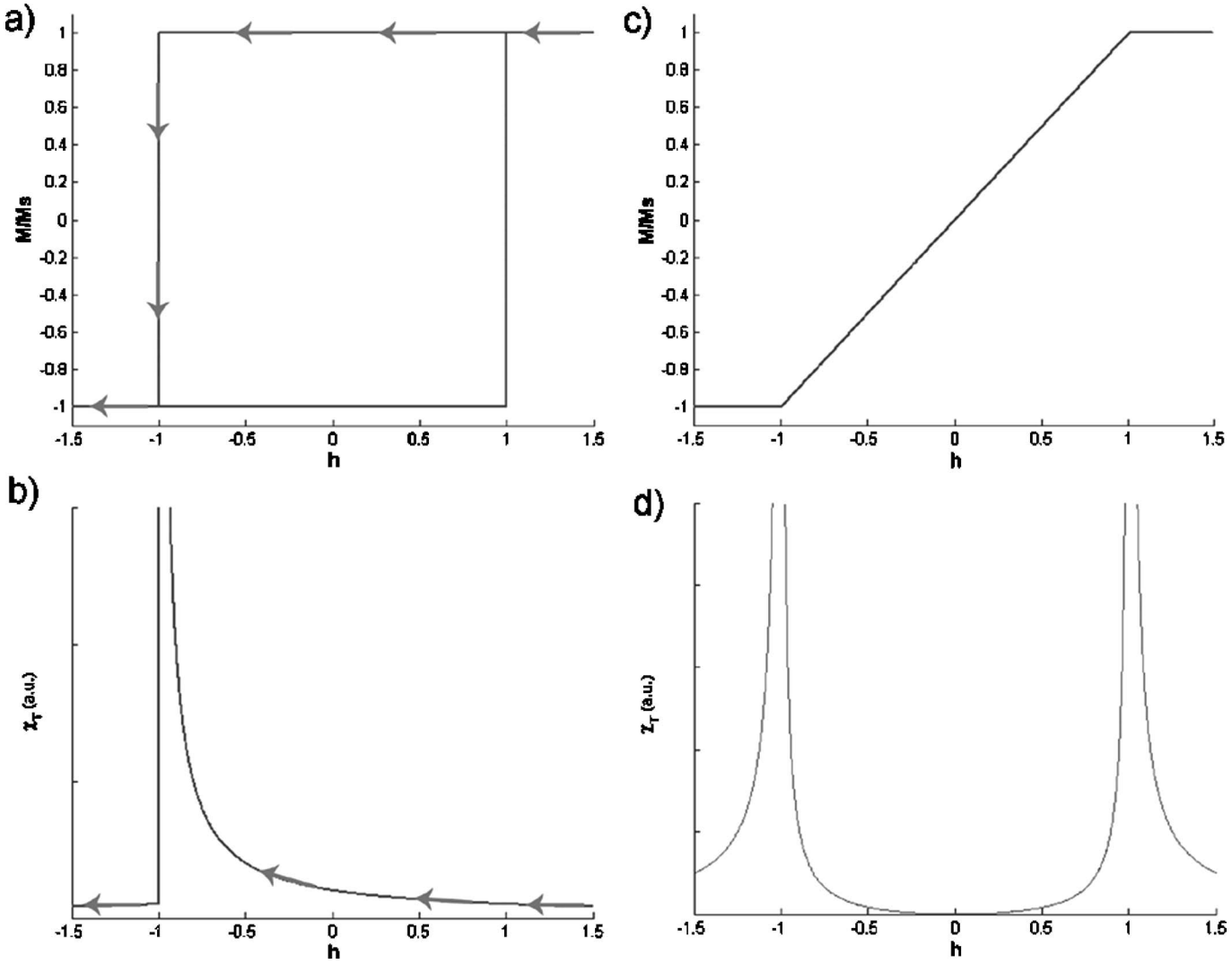

FIG. 5. Calculated hysteresis loops along the easy axis (a) and along the hard axis (c), and calculated transverse susceptibility curves with the bias field H along the easy axis (b) and along the hard axis (d) for a single domain particle with uniaxial anisotropy field H_k. Only coherent rotation processes have been taken into account in the calculations. In (a) and (b) the arrows indicate the sense of the applied field. The abscissa is the normalized field $h=H_1/H_k$ for the hysteresis loop and $h=H/H_k$ for the transverse susceptibility.

TS are observed for $H=\pm H_{\text{sat}}$, where H_{sat} is the saturation field which, in the case of a single domain particle, equals the anisotropy field. H_{sat} provides an estimation of the effective macroscopic anisotropy field, which is an average over the whole sample of the anisotropy fields of all the particles, and the TS does not depend linearly on H above saturation, but follows a more complicated behavior.[24–27] The value of H_{sat} and the shape of the peaks depend strongly on the anisotropy dispersion,[25,26] on the interparticle interaction,[27,28] and on texture.[25,26] It is remarkable that in the case of identical noninteracting particles H_{sat} coincides with the value of H_k of each particle.

We have performed TS measurements from saturation with H pointing in one sense ($H>0$) to saturation with H pointing in the opposite sense ($H<0$) through $H=0$. Let us first consider the TS measurement results obtained for the fcc Co samples, i.e., Al/100 Å Co/MgO, Al/20 Å Co/MgO, and Al/15 Å V/20 Å Co/MgO. TS measurements for all these systems show a fourfold symmetry, as expected for fcc Co, with two in-plane easy magnetization axes and two in-plane hard magnetization axes alternatively at 45°. This magnetic anisotropy could not be observed in the hysteresis loops for the samples with 20 Å of Co, as mentioned in the previous section. This clearly shows that TS measurements are much more sensitive than the hysteresis loops for detecting the magnetic anisotropy. Two different behaviors have been observed depending on the Co layer thickness. The two films with 20 Å Co exhibit a very similar behavior. In Fig. 6(a) we show the TS measurements for samples Al/20 Å Co/MgO and Al/15 Å V/20 Å Co/MgO with H along the $[110]_{\text{MgO}}$ direction—Co easy axis—and with H along the $[1\bar{1}0]_{\text{MgO}}$—another Co easy magnetization axis. Figure 6(b) displays TS measurements with H along the $[100]_{\text{MgO}}$ direction—Co hard axis. The TS curves with H along the other Co hard magnetization axis were identical to those of Fig. 6(b). The maxima about $-H_c$ are broadened, which shows that the magnetization reversal takes place over a wide range of field values. From Fig. 6(a) we can estimate the range of field values over which the magnetization re-

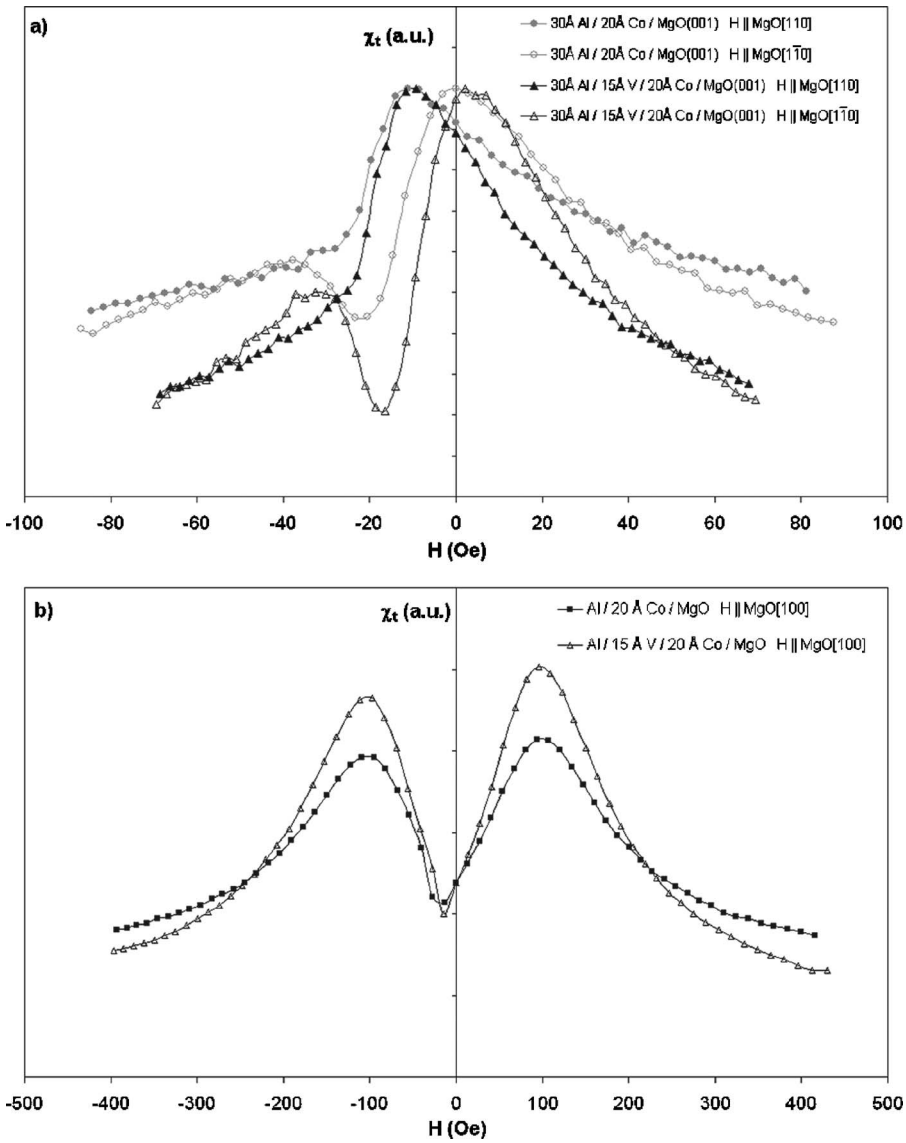

FIG. 6. Transverse susceptibility as a function of H for the samples Al/20 Å Co/MgO and Al/V/20 Å Co/MgO with H along the $[110]_{MgO}$ and $[1\bar{1}0]_{MgO}$ directions (a) and with H along the $[100]_{MgO}$ direction (b).

verses, which agree with those obtained from the Kerr hysteresis loops of Fig. 4: in the range of 10–25 Oe for H along the $[110]_{MgO}$ direction and in the range of 0–40 Oe for H along the $[1\bar{1}0]_{MgO}$ direction for both samples [see Fig. 6(a)]. In Fig. 6(a) we can also see that the TS signal associated with the magnetization reversal along the magnetization easy axis takes place for smaller magnetic fields for the film with the V capping layer. It is remarkable that, according to TS measurements, the two easy axes are not equivalent, since in the case of H along the $[1\bar{1}0]_{MgO}$ a minimum in the TS signal is observed, whereas it is absent for H applied along the $[110]_{MgO}$ direction. This minimum is due to an alignment of the magnetization along the $[110]_{MgO}$ direction during the magnetization reversal process along the $[1\bar{1}0]_{MgO}$. A similar behavior has also been observed in Fe grown on MgO (Ref. [29] and later explained as due to a superimposed uniaxial anisotropy.[30] Regarding the TS measurements with H along the $[100]_{MgO}$ direction, shown in Fig. 6(b), both films exhibit a very similar behavior. In this case, the inverse of the TS (not shown) does not depend linearly on H. On the other hand, the value of $H_{sat}=100$ Oe, determined by Co anisotropy, is the same for both films. Moreover, the peaks about $H=\pm H_{sat}$ are not sharp, but rounded. All these results suggest again a discontinuous growth of Co for this thickness, as already pointed out in the previous section.

In Fig. 7 we show the inverse of the TS for the Al/100 Å Co/MgO sample. In this case, the inverse of the TS depends linearly on H for high H values, for which the sample is saturated. This feature shows that this film is continuous. Moreover, the magnetization reversal for H along the Co magnetization easy axes (the $[110]_{MgO}$ direction) takes place very abruptly. In this case, we also performed TS measurements for H around H_c, as in Figs. 6(a) (not shown). From these measurements we could estimate that the magnetization completely reversed over a rage smaller than 3 Oe. As can be seen, the two easy axes are not equivalent either, and the inverse of the TS signal when H is applied along the $[1\bar{1}0]_{MgO}$ shows a sharp peak (which corresponds to a sharp minimum in the direct TS), as in the previous cases. For H parallel to $[100]_{MgO}$, we obtained $H_{sat}=230$ Oe which is higher than for the previous two thinner films, due to an increase of the magnetic anisotropy. In the case of this

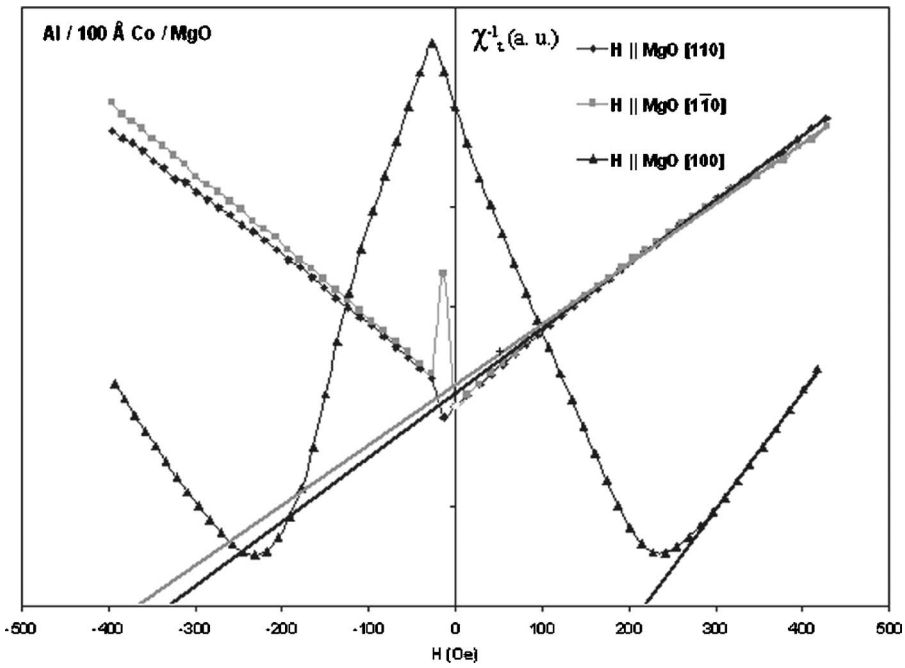

FIG. 7. Inverse of the transverse susceptibility as a function of H for the sample Al/100 Å Co/MgO with H along the $[110]_{MgO}$, $[1\bar{1}0]_{MgO}$, and $[100]_{MgO}$ directions.

sample a quantitative analysis of the anisotropies involved in the system has been carried out and is given in Sec. IV.

Let us now consider the TS measurements for the hcp Co, i.e., Al/Co/V/MgO samples. For these systems, two behaviors have been observed depending on the Co layer thickness. While all the samples exhibited an in-plane magnetic anisotropy with a fourfold symmetry, no difference was observed between the two easy magnetization axes in the TS measurements. In Fig. 8 we show the TS for the sample Al/20 Å Co/V/MgO(100). The saturation field for H applied along the hard magnetization axis can be estimated to be 250–260 Oe. The magnetization reversal for H along an easy axis takes place over a wide range of H values, between 11 and 35 Oe. In Figs. 9(a) and 9(b) the TS measurements for the sample with a thicker Co layer, Al/200 Å Co/V/MgO(100), are shown. The behavior for the sample Al/100 Å Co/MgO was similar to this one. Neither of the samples could be saturated in our experimental setup (the maximum attainable magnetic field is H_{max}=430 Oe) for H applied along the $[100]_{MgO}$ direction, which is a hard magnetization axis [see the inset in Fig. 9(a)]. The TS curves in Fig. 9(a) correspond to the H values between the two saturation peaks [see, for comparison, Fig. 6(b)]. The most striking feature in this case is the asymmetry of TS measurements for H along the hard magnetization axis. This asymmetry, which was not observed in the Kerr hysteresis loops is clearly observed in TS measurements for this sample. On the other hand, when H is applied along the $[110]_{MgO}$, which is an easy axis, a symmetric TS curve was obtained, as shown in Fig. 9(b). This result is in agreement with the symmetric Kerr hysteresis loop. The origin of this asymmetry in the first case is discussed in the next section.

IV. DISCUSSION

We can see from the above experimental results that both the structural and the magnetic properties of the systems un-

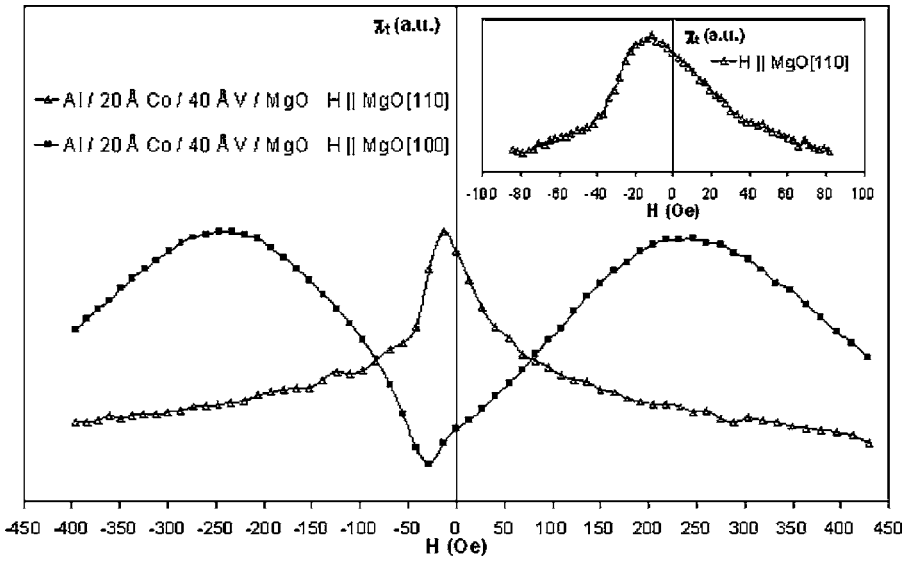

FIG. 8. Transverse susceptibility as a function of H for the sample Al/20 Å Co/40 Å V/MgO with H along the $[110]_{MgO}$ and $[110]_{MgO}$ directions. The inset shows a detailed view of the measurement along the $[110]_{MgO}$ direction around H=0.

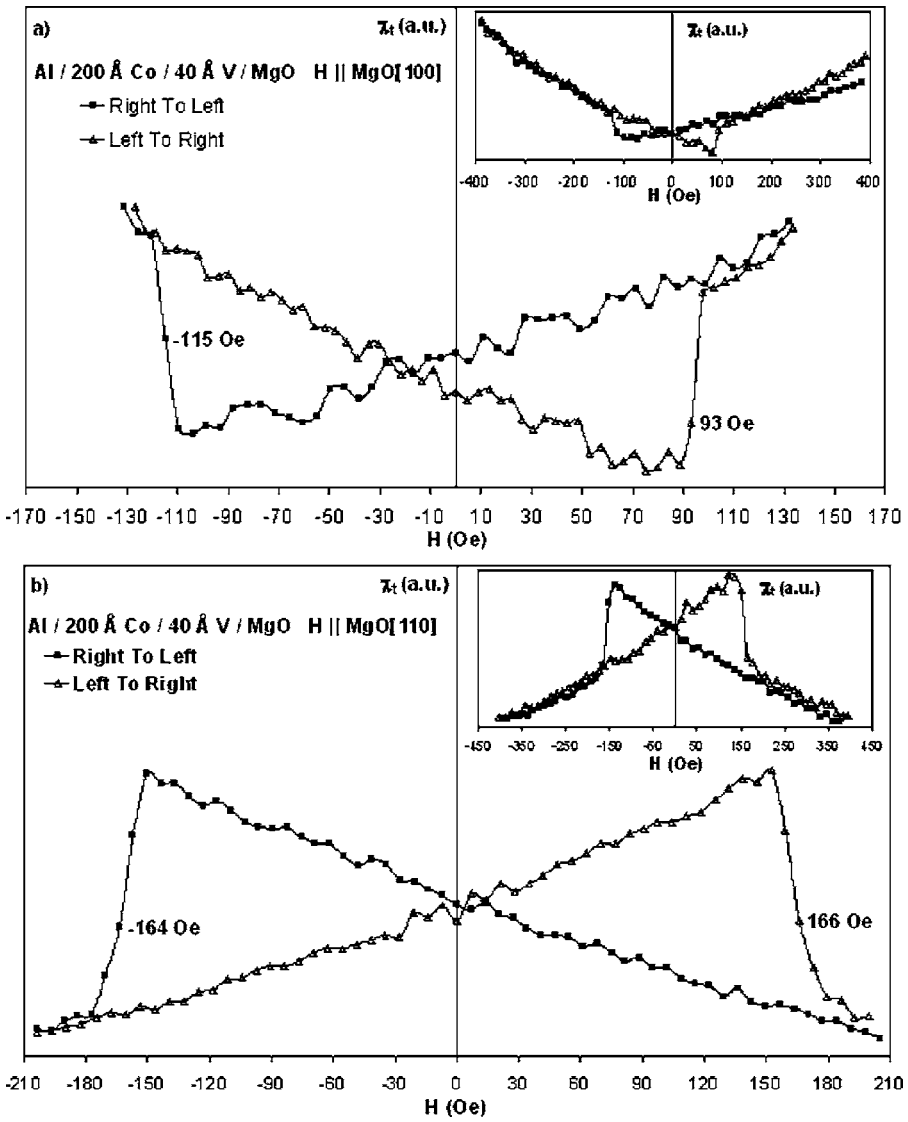

FIG. 9. Transverse susceptibility as a function of H for the sample Al/200 Å Co/40 Å V/MgO with H along the $[100]_{MgO}$ direction (a) and the $[110]_{MgO}$ direction (b).

der study basically depend on the order of deposition of Co and V on MgO(100), leading to fcc Co in V/Co/MgO(100) or to hcp Co in Co/V/MgO(100) stuctures.

Let us first consider the V/Co/MgO system. The magnetic properties in this case are determined by the Co layer and the Co/MgO(100) interface, since the subsequent deposition of the V layer leads only to very small changes. Some features are common to all the samples under study: (1) the fcc Co (001) growth exhibits the expected fourfold magnetic anisotropy (only observed with TS for the thinner samples) and (2) the Co/MgO interface seems to induce a uniaxial in-plane magnetic anisotropy. However, some differences are observed depending on the Co layer thickness and on the deposition of a V layer on Co.

Regarding the Co layer thickness, we conclude that the V/Co/MgO system develops the expected fourfold magnetic anisotropy when increasing the Co layer thickness. TS measurements for the samples with 20 Å Co are typical of a discontinuous film, and the fourfold anisotropy is not very well defined. The peaks for H applied along the $[100]_{MgO}$ direction are rounded [see Fig. 6(b)], which indicates that the magnetic saturation along that direction takes place over a wide range of H values due to the dispersion of anisotropy field values, associated with the discontinuous nature of the sample.[24,25]. Effectively, in this case, the local anisotropy field of each island is not only determined by the magnetocrystalline anisotropy but also by its shape, and a contribution from stress is expected as well. So each fcc Co island reverses the magnetization at a different H value. If we take[31] the saturation magnetization of Co as $M_s(\text{fcc}) = M_s(\text{hcp}) = 1430$ emu/cm^3, and suppose that the saturation field H_{sat} equals the anisotropy field H_1 of each Co island ($H_1 = H_{sat} = 100$ Oe), we obtain an anisotropy constant for each Co particle of $K_1 \sim 7 \times 10^4$ ergs/cm^3. Reported values[32,33] of the magnetocrystalline anisotropy of fcc Co, K_{1fcc}, range from -3.0×10^5 to -7.0×10^5 erg/cm^3 for thicknesses from 100 to 1000 Å. The absolute value estimated is much lower than the magnetocrystalline anisotropy constant for fcc Co. This can be explained if we consider that the magnetic anisotropy of the islands is highly influenced by shape and stress at this early stage of growth, and is also due to the anisotropy field dispersion and to the interisland interaction.[26–28] On the other hand, the sample with 100 Å Co shows a clearly developed fourfold magnetic anisotropy with the easy axis along the $\langle 110 \rangle_{Co}$ directions, as expected.

Therefore these results suggest that the Co layer is discontinuous at low coverages and becomes continuous at higher coverages, leading to the expected fourfold magnetic anisotropy at 100 Å. The saturation field increases with increasing Co layer thickness, which also indicates that the fourfold magnetic anisotropy value also increases as the Co layer thickness increases. In fact, the macroscopically observed anisotropy tends to that of bulk fcc Co as we will show in the case of the film with 100 Å of Co.

The superimposed uniaxial magnetic anisotropy is only manifested in the TS measurements, and as a consequence of it the two easy axes are not equivalent. It clearly affects the magnetization reversal along the $[1\bar{1}0]_{MgO}$ direction in the range of investigated Co thicknesses. This uniaxial magnetic anisotropy has also been found in fcc Co grown on MgO (Ref. 13) and on Fe grown on MgO (Ref. 23) and it is probably induced by steps in the MgO substrate surface.[34]

In the case of the film with 100 Å of Co we can calculate the fourfold anisotropy field H_{1fcc}, the ratio of the uniaxial anisotropy constant to the fourfold anisotropy constant $r = K_u/K_{1fcc}$, and the angle α between the $[100]_{Co}$ axis and the uniaxial easy axis following a formalism previously developed.[23] When applying this formalism, we have to take into account that for fcc Co, the easy axis is along the $\langle 110 \rangle$ directions, i.e., the fourfold anisotropy constant $K_{1fcc} < 0$, and that we call β the angle between the applied dc field during TS measurements and the $[100]_{Co}$ axis. In Fig. 7, $\beta = 0$ corresponds to the measurement with $H \| [100]_{MgO}$, $\beta = \pi/4$ corresponds to the measurement with H $H \| [110]_{MgO}$ and $\beta = 3\pi/4$ corresponds to the measurement with $H \| [1\bar{1}0]_{MgO}$. The linear extrapolations in Fig. 7 cut the abscissa at magnetic field values of $H(0)$, $H(\pi/4)$, and $H(3\pi/4)$ given by

$$H(0) = -H_{1fcc} - H_{1fcc} r \cos 2\alpha, \tag{1a}$$

$$H(\pi/4) = H_{1fcc} - H_{1fcc} r \sin 2\alpha, \tag{1b}$$

$$H(3\pi/4) = H_{1fcc} + H_{1fcc} r \sin 2\alpha. \tag{1c}$$

From Eqs. (1a)–(1c) we obtained $H_{1fcc} = 348$ Oe (absolute value), $r = -0.37$, and $\alpha \approx 4° \pm 1°$. With the value of M_s given above we obtained a fourfold anisotropy constant $K_{1fcc} = -2.5 \times 10^5$ erg/cm^3, close to the reported values.[32,33] The easy axis of the superimposed uniaxial anisotropy lies 4° from the $[100]_{Co}$, i.e., 4° from the $[100]_{MgO}$, in agreement with the case of Fe/MgO in which the superimposed uniaxial easy axis was found to lie 5° from the $[100]_{MgO}$.[23] This result is likely to confirm the hypothesis that the superimposed uniaxial anisotropy has a contribution from the MgO substrate.

As for the role of the V layer, it is noteworthy that the magnetization reverses in a narrower field range and for smaller field values for the film with a V layer on top [see Fig. 6(a)). This effect could be attributed to magnetic polarization of V which improves the magnetic contact between the Co islands, favoring the magnetization reversal process. Induced V magnetic moments at a V/Co interface have already been experimentally confirmed[5] and theoretically predicted.[35] V–Co intermixing, reducing the overall magnetic anisotropy of the system, and therefore the coercive field, might be an alternative interpretation.

Let us now consider the Co/V/MgO system. In this case the system is grown following the in-plane epitaxial relations $Co_{hcp}[c] \| V(001)_{bcc}[100] \| MgO(001)[110]$ and $Co_{hcp}[c] \| V(001)_{bcc}[100] \| MgO(001)[1\bar{1}0]$ All the samples showed a magnetic anisotropy with a fourfold symmetry, indicating that the hcp consists of equal volumes of material with easy axes at 90°. We can consider the films as made up of crystalline domains with the c axis along one direction and of crystalline domains with the easy axis at 90° randomly distributed over the whole surface of the sample. The two easy axes lie along the Co hcp c axes, i.e., along the $[110]_{MgO}$ and $[1\bar{1}0]_{MgO}$ directions. The hard axes lie 45° from the c axis orientations, i.e., along the $[100]_{MgO}$ and $[010]_{MgO}$ directions. The behavior of the system depends again on the Co layer thickness.

The sample with the 20 Å Co layer can be saturated along both the hard and the easy axes, as can be seen in Fig. 8. However, in both cases the TS results show a behavior typical of a nanostructured system with a great dispersion of magnetic anisotropy values.[23–25] As in the case of fcc Co, the peaks for H applied along the $[100]_{MgO}$ direction are rounded (see Fig. 8), which indicates that the magnetic saturation along that direction takes place over a wide range of H values. This result suggests that the Co layer is not continuous. Since the sample can be saturated in the range of 250–260 Oe, we can conclude that the magnetization reversal along the hard axes is not governed by the magnetocrystalline anisotropy of hcp Co. In such a case, the peaks of the TS would be detected at a magnetic field value equal to the anisotropy field of hcp Co. If we take[36] $K_{1,hcp} = 4.1 \times 10^6$ ergs/cm^3 and M_s (hcp) = 1430 emu/cm^3 we obtain an anisotropy field $H_{1,hcp} \sim 6000$ Oe and the sample could not have been saturated in our experimental setup. On the other hand, the samples with the 100 and 200 Å Co layers could only be saturated along the easy axes, but not along the hard axes. So the magnetization process along the hard axes may be controlled by the Co hcp magnetocrystalline anisotropy for the thicker samples. These results suggest that, as in the case of fcc Co, the magnetic anisotropy at the very early stages of growth is greatly influenced by some factors such as stress and shape.

According to Fig. 9(b), the magnetization reversal along the magnetization easy axes takes place in one step, and the samples are saturated along these directions and the hysteresis loops and the TS measurements are symmetric. However, the reversal along the hard axes needs a more careful inspection. The asymmetry in the TS measurements along the hard axes for the samples with 100 and 200 Å Co is associated with the fact that these samples are not saturated, as deduced from TS measurements. The magnetization reversal in this case takes place in two steps, but only one of them is observed in the range of field values attained in our experimental setup. A detailed study of this phenomenon is out of the scope of this paper and is still under investigation.

V. CONCLUSIONS

We have investigated the crystallographic structure, the magnetic anisotropy, and the magnetization reversal of the V/Co/MgO and Co/V/MgO structures. Cobalt grows in the fcc structure on MgO(100). Vanadium grows in the bcc structure on MgO and Co in the hcp structure on V with two hcp crystalline domains with the *c* axis on the plane but rotated 90° to each other. Although the expected fourfold symmetry of the anisotropy for fcc Co is already observed for a thickness of Co of 20 Å, its value is too low to be exclusively attributed to Co magnetocrystalline anisotropy. For a thickness of 200 Å of Co the anisotropy observed is close to the bulk value. In the case of hcp Co fourfold anisotropy is also already observed for a thickness of Co of 20 Å. However, the observed value is again too low compared to that of the magnetocrystalline anisotropy of hcp Co. In both cases and in the early stages of growth, the Co layer is not continuous and the magnetic anisotropy macroscopically observed is influenced by stress and shape anisotropies. Deposition of a vanadium layer onto the fcc Co layer induces a slight decrease of the coercive field and favors the magnetization reversal.

ACKNOWLEDGMENTS

The Spanish Commission of Science and Technology (CICyT) is acknowledged for financial support. One of the authors (Y.H.) acknowledges the Ramón y Cajal program and Consejo Superior de Investigaciones Científicas (CSIC) for financial support. Another author (B.P.) acknowledges Plan Investigación, Desarrollo Tecnológico e Innovación de Asturias 2001–2004 for financial support.

[1] S. S. P. Parkin, Phys. Rev. Lett. **67**, 3598 (1991).
[2] R. Krishman, T. Catinaud, M. Seddat, M. Porte, and M. Tessier, J. Magn. Magn. Mater. **159**, 175 (1996).
[3] J. Du, M. Lu, L. N. Tong, W. Ji, H. R. Zhai, and H. Xia, J. Magn. Magn. Mater. **177–181**, 1209 (1996).
[4] Y. Huttel, G. van der Laan, T. K. Johal, N. D. Telling, and P. Bencok, Phys. Rev. B **68**, 174405 (2003).
[5] B. Heinrich and J. F. Cochran, Adv. Phys. **42**, 523 (1993); H. Fritzsche, J. Kohlepp, H. J. Elmers, and U. Gradmann, Phys. Rev. B **49**, 15665 (1994); *Ultrathin Magnetic Structure I*, edited by J. A. C. Bland and B. Heinrich (Springer, Berlin, 1994).
[6] Y. Huttel, E. Navarro, and A. Cebollada, J. Cryst. Growth **273**, 474 (2004).
[7] C. K. Lo, I. Klik, Y. Liou, C. P. Chang, C. S. Yang, and Y. D. Yao, J. Magn. Magn. Mater. **177–181**, 1257 (1998).
[8] Y. Ikuhara, Y. Sugawara, I. Tanaka, and P. Pirouz, Interface Sci. **5**, 5 (1997).
[9] Y. Ikuhara and P. Pirouz, Microsc. Res. Tech. **40**, 206 (1998).
[10] M. Gutsche, H. Kraus, J. Jochum, B. Kemmather, and G. Gutekunst, Thin Solid Films **248**, 18 (1994); M. Gutsche, H. Kraus, J. Jochum, and B. Kemmather, Superconductivity and Superconducting Materials Technologies: Proceedings of Topical Symposium IV on Superconductivity, 1995 (unpublished), pp. 187–194.
[11] M. Hashimoto, H. Qiu, T. Ohbuchi, M. Adamik, H. Nakai, A. Barna, and P. B. Barna, J. Cryst. Growth **166**, 792 (1998).
[12] Y. D. Yao, Y. Liou, J. C. A. Huang, S. Y. Liao, I. Klik, C. P. Chang, and C. K. Lo, IEEE Trans. Magn. **32**, 4669 (1996).
[13] C. K. Lo, Y. Liou, C. P. Chang, I. Klik, Y. D. Yao, and J. C. A. Huang, Appl. Phys. Lett. **68**, 2155 (1996).
[14] C. K. Lo, I. Klik, C. P. Chang, Y. Liou, C. S. Yang, Y. D. Yao, and J. A. C. Huang, Appl. Surf. Sci. **113**, 160 (1997).
[15] Q. Jiang, H.-N. Yang, and G.-C. Wang, Surf. Sci. **373**, 181 (1997).
[16] I. Klik, U. M. Chen, Y. D. Yao, C. K. Lo, C. P. Chang, S. Y. Liao, and Y. Liou, Appl. Surf. Sci. **113**, 165 (1997).
[17] Y. Z. Wu, H. F. Ding, C. Jing, D. Wu, G. S. Dong, X. F. Jin, K. Sun, and S. Zhu, J. Magn. Magn. Mater. **198**, 297 (1999).
[18] E. C. Stoner and E. P. Wohlfarth, Philos. Trans. R. Soc. London, Ser. A **240**, 599 (1948).
[19] K. L. Chopra, *Thin Film Phenomena* (McGraw-Hill, New York, 1969), pp. 654–659.
[20] H. Hoffmann, Phys. Status Solidi **33**, 175 (1969).
[21] M. C. Contreras, J. F. Calleja, M. Rivas, M. O. Gutiérrez, and J. A. Corrales, J. Magn. Magn. Mater. **175**, 64 (1997).
[22] A. Stancu and L. Spinu, J. Magn. Magn. Mater. **266**, 200 (2003).
[23] J. F. Calleja, J. L. Menéndez, A. Cebollada, and C. Contreras, Jpn. J. Appl. Phys., Part 1 **40**, 6829 (2001).
[24] L. Paretti and G. Turilli, J. Appl. Phys. **61**, 5098 (1987).
[25] P. Poddar, J. L. Wilson, H. Srikanth, D. F. Farrell, and S. A. Majetich, Phys. Rev. B **68**, 214409 (2003).
[26] A. Hoare, R. W. Chantrell, W. Schmitt, and A. Eiling, J. Phys. D **26**, 461 (1993).
[27] R. Matarranz, M. C. Contreras, G. Pan, B. Presa, J. A. Corrales, and J. F. Calleja, J. Appl. Phys. **99**, 08Q504 (2006).
[28] Ch.-R. Chang and J.-S. Yang, Appl. Phys. Lett. **65**, 496 (1994).
[29] C. Contreras, J. L. Menéndez, A. Cebollada, and J. F. Calleja, Jpn. J. Appl. Phys., Part 1 **38**, 106 (1999).
[30] C. Martínez Boubeta, A. Cebollada, J. F. Calleja, C. Contreras, F. Peiró, and A. Cornet, J. Appl. Phys. **93**, 2126 (2003).
[31] H. P. Oepen, M. Benning, H. Ibach, C. M. Schneider, and J. Kirschner, J. Magn. Magn. Mater. **86**, L137 (1990).
[32] T. Suzuki, D. Weller, C. A. Chang, R. Savoy, T. Huang, B. A. Gurney, and V. Speriosu, Appl. Phys. Lett. **64**, 2736 (1994).
[33] J. A. Wolf, J. J. Krebs, and G. A. Prinz, Appl. Phys. Lett. **65**, 1057 (1994).
[34] C. Martínez Boubeta, C. Clavero, J. M. García-Martín, G. Armellas, A. Cebollada, Ll. Balcells, J. L. Menéndez, F. Peiró, A. Cornet, and M. F. Toney, Phys. Rev. B **71**, 014407 (2005).
[35] T. A. Carillo-Cázares, S. Meza-Aguilar, and C. Demangeat, J. Magn. Magn. Mater. **290/291**, 110 (2005); T. A. Carrillo-Cázares, S. Meza-Aguilar, and C. Demangeat, Eur. Phys. J. B **48**, 249 (2005); J. Hong, J. Magn. Magn. Mater. **303**, 191 (2006).
[36] R. C. O'Handley, *Modern Magnetic Materials: Principles and Applications* (Wiley, New York, 2000).